

Atmosphere of Callisto

Mao-Chang Liang,¹ Benjamin F. Lane,² Robert T. Pappalardo,³ Mark Allen,^{1,4} and Yuk L. Yung¹

Received 11 July 2004; revised 17 October 2004; accepted 1 December 2004; published 8 February 2005.

[1] During the Galileo flybys of Callisto in 1999, a CO₂ atmosphere and an ionosphere were detected. Using the Caltech/Jet Propulsion Laboratory one-dimensional KINETICS model, we have successfully simulated the observed electron density within a factor of 2, while satisfying the observational constraints on carbon and oxygen atoms. We conclude that photoionization of CO₂ alone is insufficient to produce the observed electron density. An atmosphere 20–100 times denser than the CO₂ atmosphere must be introduced, as suggested by Kliore et al. (2002). We show that an O₂-rich atmosphere is highly probable. However, the atomic oxygen produced from O₂ photodissociation is 2 orders of magnitude greater than the upper limit given by Strobel et al. (2002). The introduction of reactive hydrogen chemistry assuming a surface abundance of H₂O of $\sim 2 \times 10^9 \text{ cm}^{-3}$ (4×10^{-8} mbar) is required to reduce the excess atomic O abundance. The calculated atomic O column density is $>5 \times 10^{12} \text{ cm}^{-2}$, which is about the observed upper limit, suggesting we should be able to detect O in the atmosphere of Callisto.

Citation: Liang, M.-C., B. F. Lane, R. T. Pappalardo, M. Allen, and Y. L. Yung (2005), Atmosphere of Callisto, *J. Geophys. Res.*, 110, E02003, doi:10.1029/2004JE002322.

1. Introduction

[2] It is now known that all four Galilean satellites have tenuous atmospheres. On Io SO₂ is derived from volcanic emission [Pearl et al., 1979; Lellouch, 1996], while O₂ on Europa [Hall et al., 1995] and atomic oxygen and hydrogen on Ganymede [Barth et al., 1997] are most likely the result of radiolysis of surface ice [Johnson, 1998]. Recently, a thin CO₂ atmosphere was discovered on Callisto [Carlson, 1999] using Near-Infrared Mapping Spectrometer data from the Galileo spacecraft. Specifically, CO₂ airglow in the ν_3 band (4.3 μm) was seen in limb-scanning observations. The measured emission was modeled as an isothermal layer at a temperature of 150 ± 50 K, and a surface pressure of 7.5×10^{-9} mbar. The inferred scale height of the atmospheric CO₂ is 23 km and the surface number density is $4 \times 10^8 \text{ cm}^{-3}$. The total column density of CO₂ is approximately $9.2 \times 10^{14} \text{ cm}^{-2}$. The stated uncertainties are 60% [Carlson, 1999].

[3] During flybys of the Galileo spacecraft in 1999, an ionosphere on Callisto was detected only at the location where the trailing hemisphere was illuminated by the Sun [Gurnett et al., 2000; Kliore et al., 2002]. The electron density is determined by measuring the delay of radio signal

between the Earth and the spacecraft, the technique of radio occultation. The inferred electron densities at 27.2 and 47.6 km are 15300 and 17400 cm^{-3} , respectively. The photoionization of CO₂ alone is insufficient to produce the observed electron density. By analogy with Europa, Kliore et al. [2002] proposed a primarily O₂ atmosphere, formed from the dissociation of H₂O sputtered from the surface [Hall et al., 1995; Johnson et al., 1998]. The estimated surface neutral density is on the order of 10^{10} cm^{-3} . However, species other than CO₂ have not been observed in the atmosphere; Strobel et al. [2002] reported upper limits of the abundances of O₂ and CO to be 10^{17} cm^{-2} and atomic carbon and atomic oxygen to be 10^{13} and $2.5 \times 10^{13} \text{ cm}^{-2}$, respectively. The latter two upper limits set strict constraints for the modeling work in this paper.

[4] In this paper we examine a range of models for the atmosphere of Callisto that can reproduce the electron densities and satisfy the upper limits of the observations of O₂, CO, O and C. The implications of the models are discussed.

2. Model Description

[5] A one-dimensional Caltech/Jet Propulsion Laboratory KINETICS model is applied to the atmosphere of Callisto (see, e.g., Gladstone et al. [1996] for details of the model). The model consists of 43 spherical layers along the radial direction from the surface to an altitude of 350 km. The bottom 5 layers are used to simulate enhanced chemistry for three-body reactions on the surface. The temperature profile is assumed to be isothermal at 150 K, and the surface pressure of CO₂ is fixed at 7.5×10^{-9} mbar [Carlson, 1999]. For this tenuous CO₂ atmosphere, the calculated electron density from CO₂ photoionization is an order of

¹Division of Geological and Planetary Sciences, California Institute of Technology, Pasadena, California, USA.

²MIT Center for Space Research, Cambridge, Massachusetts, USA.

³Laboratory for Atmospheric and Space Physics, University of Colorado, Boulder, Colorado, USA.

⁴Jet Propulsion Laboratory, California Institute of Technology, Pasadena, California, USA.

Table 1. Major Reactions

Reactants		Products	Rate Coefficients ^a	References ^b
CO + hν	→	C + O	6.2×10^{-8}	19
CO + hν	→	CO ⁺ + e ⁻	2.2×10^{-8}	10, 12, 16, 17, 26, 29
CO ₂ + hν	→	CO + O	2.9×10^{-8}	19, 30
CO ₂ + hν	→	CO + O(¹ D)	4.6×10^{-8}	19, 30
CO ₂ + hν	→	CO + O(¹ S)	1.0×10^{-7}	13, 14, 21
CO ₂ + hν	→	CO ₂ ⁺ + e ⁻	4.6×10^{-8}	2, 15, 22, 30
O ₂ + hν	→	2 O	7.3×10^{-8}	19, 30
O ₂ + hν	→	O + O(¹ D)	1.8×10^{-7}	19, 30
O ₂ + hν	→	O ₂ ⁺ + e ⁻	3.6×10^{-8}	30
O ₃ + hν	→	O ₂ + O(¹ D)	2.8×10^{-4}	30
H ₂ O + hν	→	H + OH	5.7×10^{-7}	19, 30
H ₂ O + hν	→	H ₂ O ⁺ + e ⁻	2.7×10^{-8}	19, 30
C + O ₂	→	O + CO	1.6×10^{-11}	1, 5, 8, 11, 12, 25
O + OH	→	O ₂ + H	4.9×10^{-11}	19, 30
O(¹ D) + CO ₂	→	O + CO ₂	$7.4 \times 10^{-11} e^{120/T}$	30
O(¹ D) + O ₂	→	O + O ₂	$3.2 \times 10^{-11} e^{70/T}$	30
O(¹ D) + H ₂ O	→	2 OH	2.2×10^{-10}	4, 19, 30
O(¹ S) + M	→	O + M	1.0×10^{-10}	estimate
CO + OH	→	CO ₂ + H	1.5×10^{-13}	19, 30
CO ⁺ + O ₂	→	CO + O ₂ ⁺	3.1×10^{-10}	18
CO ₂ ⁺ + e ⁻	→	CO + O	4.0×10^{-7}	6, 7, 24, 28, 30
O ₂ ⁺ + e ⁻	→	2 O	3.2×10^{-7}	23, 30
H ₂ O ⁺ + O ₂	→	H ₂ O + O ₂ ⁺	4.6×10^{-7}	31
H ₂ O ⁺ + e ⁻	→	O + 2 H	2.9×10^{-7}	3, 20, 27
H ₂ O ⁺ + e ⁻	→	O + H ₂	4.7×10^{-8}	3, 20, 27
H ₂ O ⁺ + e ⁻	→	OH + H	8.9×10^{-8}	3, 20, 27
O + O ₂ + M	→	O ₃ + M	$1.8 \times 10^{-27} T^{-2.62}$	9, 19, 30
H + O ₂ + M	→	HO ₂ + M	1.7×10^{-31}	4, 30
O + HO ₂	→	OH + O ₂	1.1×10^{-10}	4, 30
OH + HO ₂	→	H ₂ O + O ₂	2.5×10^{-10}	4, 30

^aUnits are s⁻¹ for photolysis reactions, cm³ s⁻¹ for two-body reactions, and cm⁶ cm⁻¹ for three-body reactions. The photolysis rate coefficients are given at the top of the model atmosphere.

^bReferences: 1, *Brion and Carnovale* [1985]; 2, *Chan et al.* [1993]; 3, *Datz et al.* [2000]; 4, *DeMore et al.* [1997]; 5, *Dutuit et al.* [1985]; 6, *Gougousi et al.* [1997]; 7, *Gutcheck and Zipf* [1973]; 8, *Haddad and Samson* [1986]; 9, *Hippler et al.* [1990]; 10, *Huber and Herzberg* [1979]; 11, *Katayama et al.* [1973]; 12, *Kronebush and Berkowitz* [1976]; 13, *Lawrence* [1972a]; 14, *Lawrence* [1972b]; 15, *Masuoka* [1994]; 16, *Masuoka and Nakamura* [1993]; 17, *Masuoka and Samson* [1981]; 18, *Miller et al.* [1984]; 19, see references of *Moses et al.* [2000]; 20, *Mul et al.* [1983]; 21, *Okabe* [1978]; 22, *Shaw et al.* [1995]; 23, *Sheehan and St.-Maurice* [2004]; 24, *Skrzypkowski et al.* [1998]; 25, *Tan et al.* [1978]; 26, *Van Brunt et al.* [1972]; 27, *Vejby-Christensen et al.* [1997]; 28, *Weller and Biondi* [1967]; 29, *Wight et al.* [1976]; 30, see references of *Yung and DeMore* [1999]; 31, *Le Teuff et al.* [2000].

magnitude less than the measured density and peaks on the surface. Therefore a neutral atmosphere denser than CO₂ must be introduced. We believe that O₂ atmosphere is the most probable, and will examine this assumption in later sections. Such an atmosphere has been proposed by *Kliore et al.* [2002].

[6] In order to match the observed electron density, the inferred surface density of O₂ is on the order of 10¹⁰ cm⁻³, which is ~20 times denser than that of CO₂. So we adopt surface densities of ~7 × 10⁹ and 4 × 10⁸ cm⁻³ for O₂ and CO₂, respectively. The surface H₂O vapor pressure is taken to be ~4 × 10⁻⁸ mbar (2 × 10⁹ cm⁻³). For the other lower boundary conditions, we set the transport flux to be zero and let the three-body reactions to be more efficient on the surface. We adopt a rate coefficient of 10⁻²⁰ cm⁶ s⁻¹ for three-body reactions on the surface (or an effective two-body rate coefficient of 10⁻¹⁰ cm³ s⁻¹), the number chosen to reach the kinetic limit of chemical reactions. This assumption of enhanced reactions on the surface may be reasonable if the surface/regolith is porous and can adsorb particles. Actually, only H + O₂ + M → HO₂ + M will be significantly modified. We take this as our reference model, which fulfills the observational constraints to a fair accuracy. The results of relaxing the surface effect will be presented in later sections. For the upper boundary conditions, we assume the boundary is not permeable for

species other than H, H₂, and O. The H and H₂, the lightest two neutral species, are allowed to escape with Jeans escape velocities: At 150 K they are ~10⁴ and ~10³ cm s⁻¹, respectively. The escape of O atoms is mainly by sputtering of energetic ions in the Jovian magnetosphere. So the H escape will be limited by the escape of O atoms. Since the atmosphere is tenuous, we believe the diffusion is dominated by molecular diffusion. Near surface the molecular diffusion coefficient for H is on the order of 10⁹ cm² s⁻¹. Hence we omit eddy diffusion in the model.

[7] Table 1 lists the major chemical reactions in the model (minor reactions are not shown in the table). Because of a high electron density, the lifetimes of ions are ~400 s. The ions will quickly react with electrons before they diffuse away. So we assume a quasi-neutral atmosphere in our model, i.e., in each layer the electron density equals the ionic density. The electrodynamic interaction between the Callisto's ionosphere and the Jovian plasma is suggested to be minor (see *Strobel et al.* [2002] for a detailed discussion). This is also consistent with the results that there is no excess of electron density in the downstream as compared to the upstream of the plasma around Callisto [*Gurnett et al.*, 2000].

[8] The solar flux values are taken from *Mount and Rottman* [1983], *Torr and Torr* [1985], and *World Meteorological Organization* [1985], and then scaled appropri-

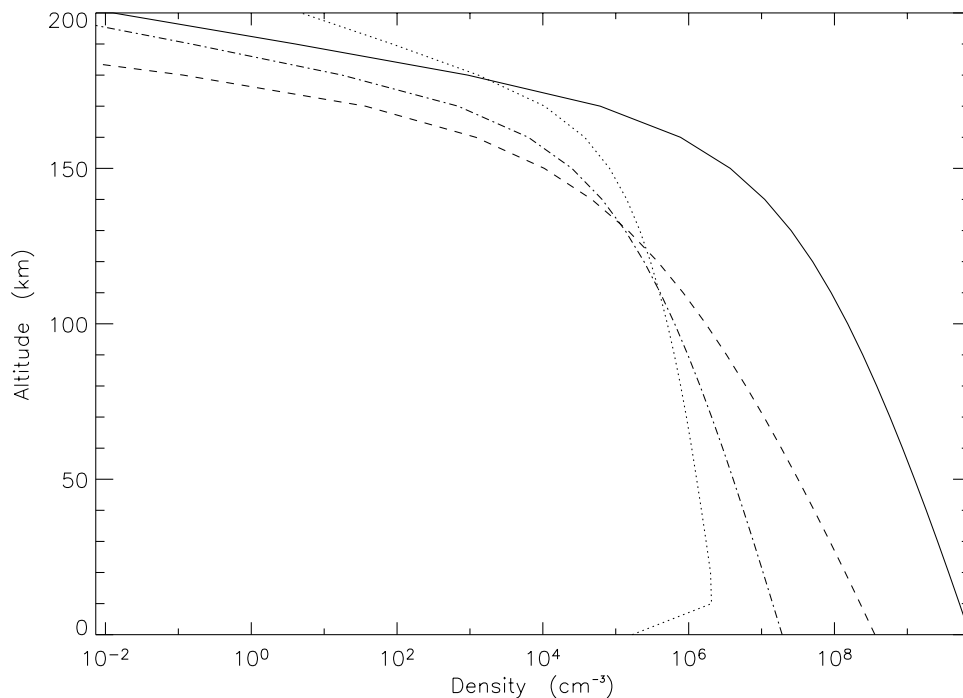


Figure 1. Vertical profiles of oxides: O₂ (solid line), O (dotted line), CO₂ (dashed line), and CO (dash-dotted line).

ately for the mean distance between the Sun and Callisto (5.2 AU). The Callisto's ionosphere was detected in 1999, when the solar cycle was close to the solar maximum (the solar cycle reached its maximum in 2000). So the solar maximum flux is adopted to be our reference solar flux. The solar zenith angle is fixed at 80°, which is the mean angle of the observation of the ionosphere. The model results with solar mean and minimum fluxes are also shown.

3. General Results

3.1. Electron Density and Hydrogen Abundance

[9] The profiles of major constituents in our calculation are plotted in Figures 1 and 2. Figure 3 shows the total photoabsorption rates for O₂, H₂O, CO₂, and CO. The branching ratios of photoionization are about ~10% that of the total (see, e.g., Table 1). Since we have assumed a quasi-neutral atmosphere, the major ion is O₂⁺ (Figure 4). There are two sources of O₂⁺: the photoionization product of the most abundant molecule, O₂, in the model and the charge exchange between H₂O⁺ and O₂. In order to better match the observed electron density profile, the required O₂ density is on the order of 10⁹ cm⁻³ at 50 km above the surface. This corresponds to an O₂ column density of 2 × 10¹⁶ cm⁻². Figure 4 shows the profiles of total electron density (dark solid line), O₂⁺ (dashed line), H₂O⁺ (dotted line), CO₂⁺ (dash-dotted line), and O⁺ (long-dashed line) during the solar flux maximum. We see that the modeled electron density agrees with the observation to within a factor of 2. Our model results support the assumption of an O₂ atmosphere on Callisto [Kliore *et al.*, 2002].

[10] The O₂⁺ is lost locally by recombination with electrons, the lifetimes being ~400 s, while its parent molecule O₂ has timescale of ~10⁷ s against photoionization. As a

result, the ions are ~10⁻⁴ as abundant as their parents. Since the UV flux is limited and the atmosphere is not optically thin at UV wavelengths, the observed electron density profile gives a strong constraint on the composition of the atmosphere on Callisto. As proposed by Kliore *et al.* [2002], H₂O, O, H₂, OH, and H all have ionization cross sections similar to O₂, and hence they are other possibilities for atmospheric constituents. Because of the low gravity (H and H₂ can escape readily), low temperature (H₂O vapor abundance is very sensitive to the temperature), and observationally constrained low O abundance [Strobel *et al.*, 2002], the assumption of an O₂ atmosphere on Callisto is the most plausible, which was also the proposed solution for the atmospheres of Ganymede and Europa [see, e.g., Hall *et al.*, 1998, and references therein].

[11] If the surface is not porous and not able to adsorb particles, the chemical reactions will not be enhanced. In this case, the electron profile is in better agreement with the measurements (see light solid line in Figure 4). The peak electron density is sensitive to solar zenith angle. Increasing the angle from 79 to 82° will move the peak upward by ~20 km; this brings the model into better agreement with the measurements [Kliore *et al.*, 2002]. The required surface densities of O₂ and H₂O are 3.2 × 10¹⁰ cm⁻³ and 4.8 × 10⁹ cm⁻³, respectively. The values are 4 times greater than those of the reference model. The reason for this is that HO₂ is now formed inefficiently on the surface and subsequent chemistry resulting in the recycling of O₂ and H₂O is negligible (last 3 reactions in Table 1). Consequently, O₂ and H₂O will be present in lower abundances in the upper atmosphere.

[12] Though the model without enhanced surface reactions can better match the electron profiles, it is unlikely, as we will discuss later. In the upper atmosphere, the ultimate

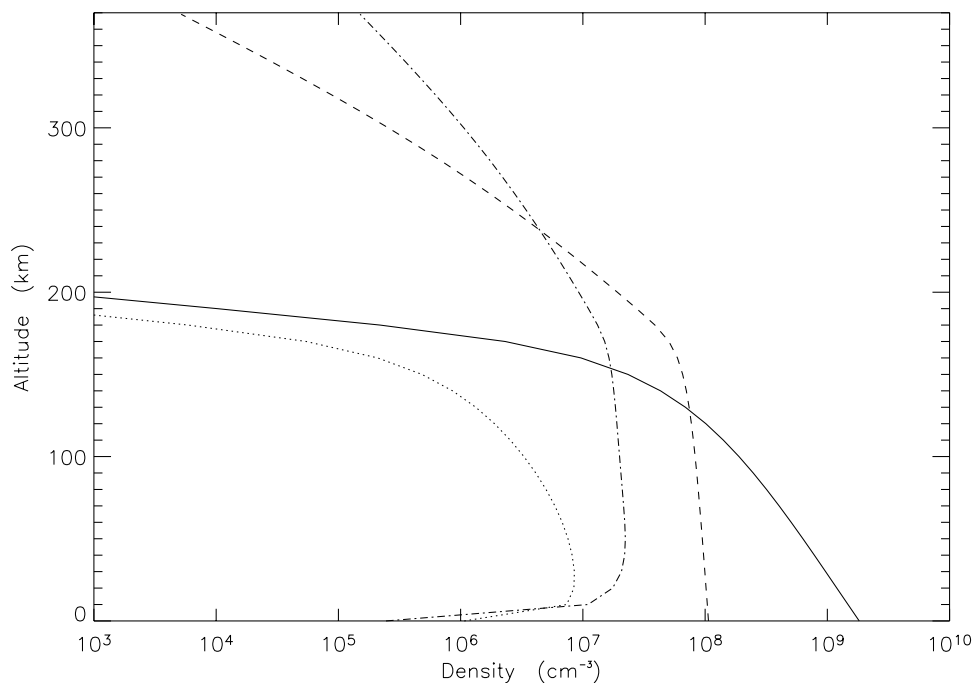


Figure 2. Vertical profiles of H₂O (solid line), OH (dotted line), H₂ (dashed line), and H (dash-dotted line).

source of electrons (or ions) is photoionization of H and H₂. The electron density is determined by the reactions between H and H₂ photoionizations and the recombination of H₂⁺ plus e⁻, and it is estimated to be $\sim 150 \text{ cm}^{-3}$ at $\sim 400 \text{ km}$ above the surface, which is a factor of ~ 4 less than the observed value of $\sim 400 \text{ cm}^{-3}$ at an altitude of 535 km

[Gurnett *et al.*, 2000]. The value is calculated by assuming a photoionization coefficient of $5 \times 10^{-9} \text{ s}^{-1}$, density of 10^5 cm^{-3} , and recombination rate coefficient of $2 \times 10^{-8} \text{ cm}^3 \text{ s}^{-1}$ [Le Teuff *et al.*, 2000]. The discrepancy can be explained by the fact that the density scale height in the upper atmosphere is significantly greater than that in the

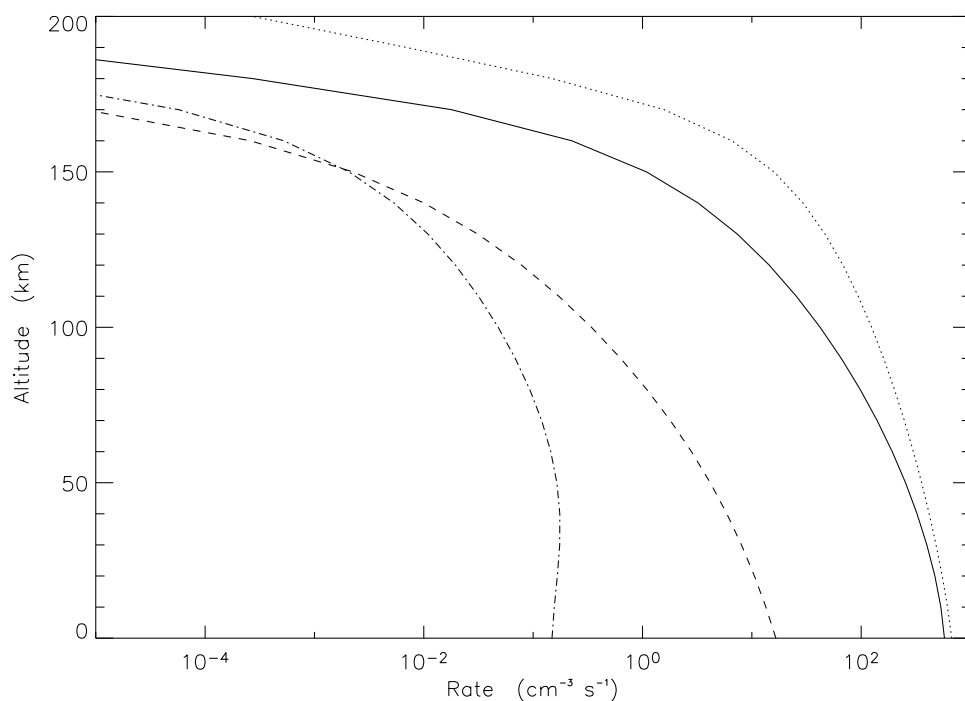


Figure 3. Vertical profiles of total photoabsorption rates for O₂ (solid line), H₂O (dotted line), CO₂ (dashed line), and CO (dash-dotted line).

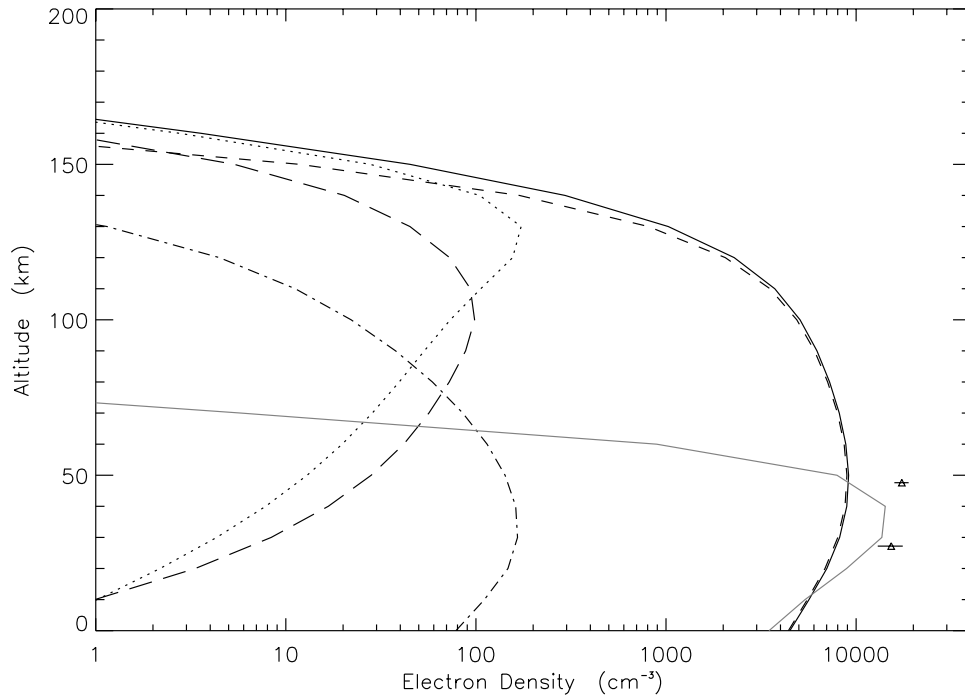


Figure 4. Vertical profiles of total electron density (dark solid line), O₂⁺ (dashed line), H₂O⁺ (dotted line), CO₂⁺ (dash-dotted line), and O⁺ (long-dashed line) in our reference model (enhanced surface chemical reactions). A model with no chemical reactions enhanced on the surface is shown for comparison (light solid line). Triangles are Galileo spacecraft flyby experiments. The reported error bars are overplotted.

lower atmosphere, because H and H₂ are the major species in the upper atmosphere. In our present model, we assume the density scale height is constant at ~ 30 km throughout the whole atmosphere.

[13] The H atoms can be lost only by the enhanced three-body reactions on the surface and by Jeans escape, because H is unreactive in the atmosphere. Therefore the H (and H₂) abundance will be high (see Table 2 and Figure 2). The abundances of H and H₂ will be extremely sensitive to the properties of the surface of Callisto. So by observing the H profile, we will be able to quantify communication processes between the surface and the atmosphere. The existence of enhanced surface reactions can also be tested

by observing the abundance of O₃. In the reference model, the abundance of O₃ is $\sim 5 \times 10^{12}$ cm⁻², while it is negligible without the enhanced surface reactions.

3.2. Carbon Dioxide and Carbon Monoxide

[14] The profiles of density and photoabsorption rates of CO₂ and CO are shown in Figures 1 and 3, respectively. CO₂ is destroyed mainly by photodissociation, and can be recycled either by the reaction of CO with OH or by the three-body reaction of O and CO under the assumption of enhanced chemical reaction rates on the surface. CO is primarily formed by the CO₂ photodissociation. In vacuum, it is shown in Table 2 that CO has a lifetime, against UV, a

Table 2. Abundances of C, O, CO, H, and H₂

	H ₂ O ^a	C ^b	O ^b	CO ^b	H ^b	H ₂ ^b
Obs. ^c	...	$<10^{13}$	$<2.5 \times 10^{13}$	$<10^{17}$
Max. ^d	0	1.8×10^8	1.6×10^{15}	4.3×10^{13}
	0.10	6.4×10^8	1.2×10^{14}	2.4×10^{14}	2.4×10^{14}	8.1×10^{14}
	0.25	1.2×10^8	1.3×10^{13}	6.0×10^{13}	3.5×10^{14}	3.2×10^{15}
	0.50	4.4×10^7	7.6×10^{12}	2.6×10^{13}	4.0×10^{14}	7.1×10^{15}
	1.00	1.5×10^7	5.6×10^{12}	1.1×10^{13}	4.6×10^{14}	1.4×10^{16}
	wet ^e	5.9×10^6	2.3×10^{13}	2.4×10^{13}	1.2×10^{17}	4.0×10^{15}
Avg. ^d	0.25	6.7×10^7	1.1×10^{13}	4.6×10^{13}	2.5×10^{14}	2.7×10^{15}
Min. ^d	0.25	2.4×10^7	8.3×10^{12}	2.8×10^{13}	1.6×10^{14}	1.8×10^{15}

^aThe near-surface H₂O vapor abundance. The values are relative to the O₂ density of 7.4×10^9 cm⁻³. A value of 0.25 is adopted as our reference model.

^bThe column-integrated density in units of cm⁻². H and H₂ are allowed to escape.

^cThe observed upper limits of column density for C, O, and CO [Strobel et al., 2002].

^dThe calculated abundances for maximum, averaged, and minimum solar fluxes.

^e“Wet” refers to the model where three-body chemical reactions are not enhanced on the surface. In this model, the best fits of O₂ and H₂O surface densities are 3.2×10^{10} and 4.8×10^9 cm⁻³, respectively.

factor of 3 longer than that of CO_2 . This gives an upper limit for the CO abundance, under the conditions that enhanced chemical reaction rates on the surface and OH radicals or H_2O vapors are absent. The photoionization products of CO_2 and CO, CO_2^+ and CO^+ , are lost mostly by electron recombination and by charge exchange with O_2 , respectively. As a result, the CO_2 , CO, CO_2^+ , and CO^+ have lifetimes of $\sim 10^7$, 10^6 , 300, and 20 s. The calculated abundance of CO is shown in Table 2.

3.3. Atomic Carbon and Atomic Oxygen

[15] The reported upper limits of the abundances of C and O strongly constrain the composition in the atmosphere of Callisto. Because of the high O_2 concentration, the C atoms have a lifetime of ~ 100 s. The calculated C atom column density is about 10^8 cm^{-2} (see Table 2). The abundance of O atoms depends on the H_2O vapor pressure in the atmosphere. The calculated profile of O using the reference model is shown in Figure 1. In the absence of H_2O in the atmosphere, the calculated O column density is about 10^{15} cm^{-2} , which is 2 orders of magnitude higher than the observed upper limit. By introducing an eddy diffusion of $10^{10} \text{ cm}^2 \text{ s}^{-1}$, the calculated O column density is about $3 \times 10^{13} \text{ cm}^{-2}$. This high eddy diffusion coefficient will move the atomic O downward and by the enhanced chemical processes on the surface O_2 can be recycled. While the abundance is still higher than the observed upper limit. Though eddy diffusion can reduce the O abundance, we argue that this assumption is not appropriate for two reasons. First, the electron density will be nearly constant below 100 km, while *Kliore et al.* [2002] observed an electron profile that increases sharply from the surface to 20–50 km. Second, the eddy velocity required is about 10% of the speed of the sound, a value that is unrealistic near the surface.

[16] By the analogy with the atmospheres of Mars and Ganymede, we introduce HO_x chemistry for removing O [McElroy and Donahue, 1972; Yung and McElroy, 1977]. With the assumption of H_2O surface abundance equal to 4×10^{-8} mbar the model O abundance drops by 2 orders of magnitude to nearly the observed upper limit. This value of H_2O is close to the saturation vapor pressure at 150 K [Yung and McElroy, 1977]. When we increase the abundance of H_2O , the O abundance is not seriously affected. The reason is that H_2O will become the major UV absorber. The results shown in Table 2 reflect this dependence. When H_2O to O_2 abundance ≤ 0.5 , a factor of 2 decrease in H_2O will result in an order of magnitude increase in O abundance. While the relation is saturated for H_2O to O_2 ratio > 0.5 . We list the model C and O column densities as well as the observed upper limits in Table 2. It is shown that in all cases the calculated O abundance is not far from the observed upper limit.

4. Discussion

[17] For the tenuous atmosphere of Callisto, the heat conduction time is about 100 s, which is significantly less than the 17-day rotational period of Callisto. Along with a low visual albedo of 0.2 on Callisto, the surface and the atmosphere near the surface at the day side would be, on average, about 150 K, consistent with an insignificance of

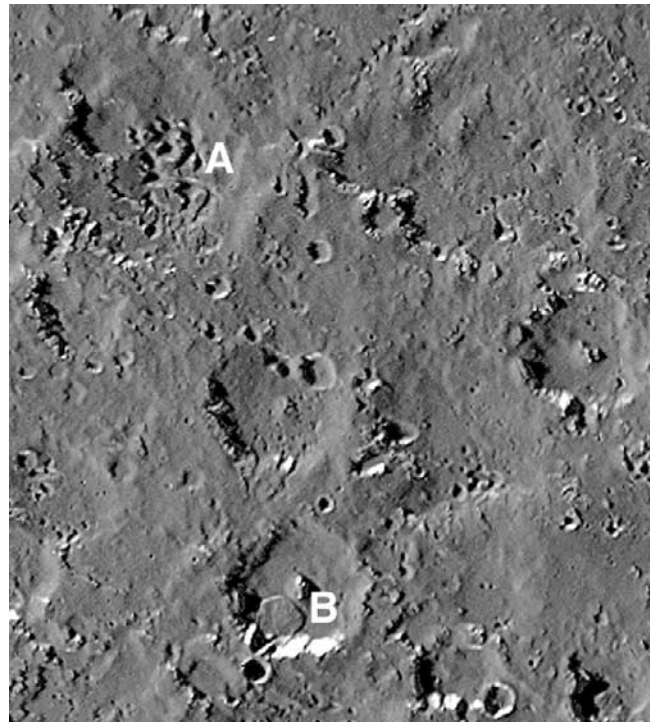


Figure 5. Callisto's surface shows abundant evidence for mass wasting of a dark mantling material. Pits (at A) suggest ground collapse due to loss of subsurface volatiles. A 4 km wide landslide deposit (at B) attests to the mobility of the dark material. Bright crater walls and local topographic highs are probably exposures of water frost cold trapped on relatively bright "bedice" which is believed to underlie the dark mantle. (Galileo Solid State Imager observation C9CSCRATER01, image s0401505526; resolution 160 m/pixel.)

condensed O_2 on the surface of Callisto [Spencer and Calvin, 2002]. This confirms that the H_2O vapor pressure of 4×10^{-8} mbar adopted by the model is reasonable.

[18] Galileo high-resolution imaging of Callisto [Moore et al., 1999] reveals that the satellite's cratered surface is dominated by smooth, dark material which appears to mantle and subdue the satellite's topography (see, e.g., Figure 5). Landslide deposits within some craters attest to the mobility of the dark material and its tendency to slough downhill off of topographic highs. High-standing crater rims, central peaks, and relatively steep interior crater walls are relatively bright. These bright areas are probably where water-ice is cold trapped, as seen by Spencer and Calvin [2002]. Callisto's craters commonly show gullied, crenulate walls, and rims which are knobby and discontinuous. Irregularly shaped pits ~ 1 km in size are observed in some regions (Figure 5), and these suggest undermining and collapse of near-surface material, as through loss of a volatile substrate.

[19] Therefore the dark areas are the likely regions that provide the required H_2O vapor pressure, and the bright regions are a probable H_2O source. Diffusion from cold to warm regions can deliver the required H_2O . In order to study the process quantitatively, we follow the approach of

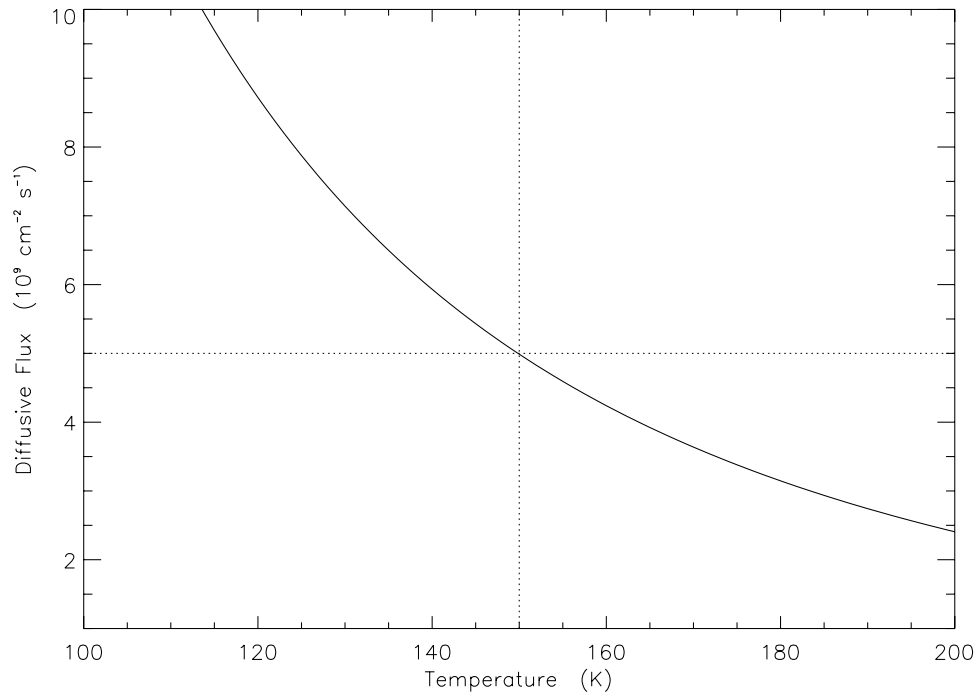


Figure 6. Profiles of H₂O diffusive flux as a function of temperature for temperature gradient of 7.7 K km⁻¹. The two dotted lines represent maximum H₂O diffusion rates (horizontal line) and the required surface temperature of 150 K (vertical line).

Moore *et al.* [1996] and applied Fick's law to model the water diffusive flux F :

$$F = D \frac{\epsilon}{\tau} \frac{\partial n(T)}{\partial x}. \quad (1)$$

Here x is the distance from the source, $n(T)$ the number density of H₂O vapor at temperature T , ϵ the porosity, and τ the tortuosity. The diffusion coefficient D is (Knudsen diffusion, i.e., dominated by gas-pore wall collisions)

$$D \approx 2\epsilon r_0 / 3\tau \sqrt{2kT/\pi m}, \quad (2)$$

where r_0 is the pore size, m the molecular mass of the diffusion component, and k the Boltzmann constant. Typically $r_0 \approx 6 \times 10^{-4}$ cm, $\epsilon \approx 0.5$, and $\tau \approx 5$ [see, e.g., Weiss *et al.*, 2000]. If we can assume a constant temperature gradient ($\partial T/\partial x$), equation (1) can be rewritten:

$$F = D \frac{\epsilon}{\tau} \frac{\partial T}{\partial x} \frac{\partial n(T)}{\partial T}. \quad (3)$$

The saturation vapor density is given by $n(T) = (kT)^{-1} \exp[-5631.120592/T + 8.231199999 \ln(T) - 0.03861573356 T + 0.00002774937399 T^2 - 15.558956661]$ cm⁻³, where T is in the unit of K [Lebofsky, 1975]. Figure 6 shows the calculated profiles of H₂O diffusive flux as a function of temperature for a temperature gradient of 7.7 K km⁻¹. Two dotted lines represents an H₂O dissociation rates of 5×10^9 cm⁻² s⁻¹ and a temperature of 150 K in our reference model. Since most of H₂O are recycled by the enhanced chemical reactions on the surface, the diffusion flux of H₂O below 5×10^9 cm⁻² s⁻¹ is the most likely. The value is determined by the loss rate of H₂O.

[20] The loss of H₂O depends on the escape of O and H atoms. H atoms can be lost easily by Jeans escape, while O atoms can be removed only by ion recombination (e.g., O₂⁺ plus e⁻) and by the sputtering of energetic ions in the Jovian magnetosphere. In the model, about 10% of O atoms are produced by the dissociative recombination of O₂⁺ plus electron. Though they may have as much as 2.5 eV per atom, or 7 km s⁻¹ (higher than the escape velocity of 2.5 km s⁻¹), they cannot escape: The exobase in the model is at about 200 km above the surface, while the energetic O atoms are produced primarily at ~50 km, where the electron density peaks. So the only loss process for O atoms is sputtering by energetic particles. The incident ion flux at Callisto's orbit is 2×10^7 cm⁻² s⁻¹ [e.g., Neubauer, 1998]. The maximum sputtering flux is calculated to be 6×10^8 cm⁻² s⁻¹ by assuming a sputtering yield of 30 [Johnson and Leblanc, 2001]. Over geological time, ~20 m of ice may be lost. This is an upper limit. Strobel *et al.* [2002] have argued that the interaction between the ionosphere of Callisto and the Jovian plasma is very limited.

[21] For the maximum sputtering flux, the H escape flux cannot be more than 10^9 cm⁻² s⁻¹. This implies that the temperature at the top of the atmosphere is <100 K. At Callisto, the maximum H₂O photolysis rate is 10^{10} cm⁻² s⁻¹. In our reference model, a significant amount of H₂O can be recycled because of enhanced recombination rates on the surface. If the surface is not porous and cannot efficiently adsorb particles, the O and H produced by H₂O photolysis must be removed from the atmosphere. Otherwise, the accumulation rate of O₂ will be large. This corresponds to an escape flux of atoms about 10^{10} cm⁻² s⁻¹, which is >2 orders of magnitude greater than that by sputtering. We propose that this hypothesis can be tested by detecting the

escape flux of O atoms and by observing the H (or H₂) abundance in the atmosphere of Callisto.

5. Summary

[22] We have modeled the photochemistry of an O₂-rich atmosphere of Callisto and have successfully reproduced the observed electron profile [Kliore *et al.*, 2002]. Because of the observational constraint on the O atom abundance [Strobel *et al.*, 2002], we propose that H₂O vapor needs to be present in the atmosphere. The OH radicals, from H₂O photolysis, will remove the O atoms, produced by O₂ photolysis. The inferred H₂O surface density is $\sim 2 \times 10^9 \text{ cm}^{-3}$ (4×10^{-8} mbar). The calculated O column density is $\sim 10^{13} \text{ cm}^{-2}$; so it should be detectable with the current instrumentation.

[23] **Acknowledgments.** We thank M. Gerstell, R. L. Shia, D. J. Stevenson, and D. F. Strobel for valuable discussions. This research was supported in part by NASA grant NAG5-6263 to the California Institute of Technology. B.F.L. gratefully acknowledges the support of a Pappalardo Fellowship in Physics of MIT.

References

- Barth, C. A., C. W. Hord, A. I. F. Stewart, W. R. Pryor, K. E. Simmons, W. E. McClintock, J. M. Aiello, K. L. Naviaux, and J. J. Aiello (1997), Galileo ultraviolet spectrometer observations of atomic hydrogen in the atmosphere of Ganymede, *Geophys. Res. Lett.*, *24*, 2147–2150.
- Brion, C. E., and F. Carnovale (1985), The absolute partial photoionization cross-section for the production of the X2b1 state of H₂O⁺, *Chem. Phys.*, *100*, 291–296.
- Carlson, R. W. (1999), A tenuous carbon dioxide atmosphere on Jupiter's moon Callisto, *Science*, *283*, 820–821.
- Chan, W. F., G. Cooper, and C. E. Brion (1993), The electronic spectrum of carbon dioxide: Discrete and continuum photoabsorption oscillator strengths (6–203 eV), *Chem. Phys.*, *178*, 401–413.
- Datz, S., R. Thomas, S. Rosen, M. Larsson, A. M. Derkatch, F. Hellberg, and W. van der Zande (2000), Dynamics of three-body breakup in dissociative recombination: H₂O⁺, *Phys. Rev. Lett.*, *85*, 5555–5558.
- DeMore, W. B., S. P. Sander, D. M. Golden, R. F. Hampson, M. J. Kurylo, C. J. Howard, A. R. Ravishankara, C. E. Kolb, and M. J. Molina (1997), Chemical kinetics and photochemical data for use in stratospheric modeling, *Eval. 12, JPL Publ. 97-4*, Jet Propul. Lab., Pasadena, Calif.
- Dutuit, O., A. Tabchehouhaile, I. Nenner, H. Frohlich, and P. M. Guyon (1985), Photodissociation processes of water vapor below and above the ionization potential, *J. Chem. Phys.*, *83*, 584–596.
- Gladstone, G. R., M. Allen, and Y. L. Yung (1996), Hydrocarbon photochemistry in the upper atmosphere of Jupiter, *Icarus*, *119*, 1–52.
- Gougousi, T., M. F. Golde, and R. Johnsen (1997), Electron-ion recombination rate coefficient measurements in a flowing afterglow plasma, *Chem. Phys. Lett.*, *265*, 399–403.
- Gurnett, D. A., A. M. Persoon, W. S. Kurth, A. Roux, and S. J. Bolton (2000), Plasma densities in the vicinity of Callisto from Galileo plasma wave observations, *Geophys. Res. Lett.*, *27*, 1867–1870.
- Gutcheck, R. A., and E. C. Zipf (1973), Excitation of CO fourth positive system by dissociative recombination of CO₂⁺ ions, *J. Geophys. Res.*, *78*, 5429–5436.
- Haddad, G. N., and J. A. R. Samson (1986), Total absorption and photoionization cross-sections of water vapor between 100-Å and 1000-Å, *J. Chem. Phys.*, *84*, 6623–6626.
- Hall, D. T., D. F. Strobel, P. D. Feldman, M. A. McGrath, and H. A. Weaver (1995), Detection of an oxygen atmosphere on Jupiter moon Europa, *Nature*, *373*, 677–679.
- Hall, D. T., P. D. Feldman, M. A. McGrath, and D. F. Strobel (1998), The far-ultraviolet oxygen airglow of Europa and Ganymede, *Astrophys. J.*, *499*, 475–481.
- Hippler, H., R. Rahn, and J. Troe (1990), Temperature and pressure dependence of ozone formation rates in the range 1–1000 bar and 90–370 K, *J. Chem. Phys.*, *93*, 6560–6569.
- Huber, K. P., and G. Herzberg (1979), *Constants of Diatomic Molecules*, p. 158, Van Nostrand Reinhold, Hoboken, N. J.
- Johnson, R. E. (1998), Sputtering and desorption from icy surfaces, in *Solar System Ices*, edited by B. Schmitt, pp. 303–334, Springer, New York.
- Johnson, R. E., and F. Leblanc (2001), The physics and chemistry of sputtering by energetic plasma ions, *Astrophys. Space Sci.*, *277*, 259–269.
- Johnson, R. E., R. M. Killen, J. H. Waite, and W. S. Lewis (1998), Europa's surface composition and sputter-produced ionosphere, *Geophys. Res. Lett.*, *25*, 3257–3260.
- Katayama, D. H., R. E. Huffman, and C. L. Obyrian (1973), Absorption and photoionization cross-sections for H₂O and D₂O in vacuum ultraviolet, *J. Chem. Phys.*, *59*, 4309–4319.
- Kliore, A. J., A. Anabtawi, R. G. Herrera, S. W. Asmar, A. F. Nagy, D. P. Hinson, and F. M. Flasar (2002), Ionosphere of Callisto from Galileo radio occultation observations, *J. Geophys. Res.*, *107*(A11), 1407, doi:10.1029/2002JA009365.
- Kronebush, P. L., and J. Berkowitz (1976), Photodissociative ionization in the 21–41 eV region: O₂, N₂, CO, NO, CO₂, H₂O, NH₃, and CH₄, *Int. J. Mass Spectrosc. Ion Phys.*, *22*, 283–306.
- Lawrence, G. M. (1972a), Production of O(1S) from photodissociation of CO₂, *J. Chem. Phys.*, *57*, 5616.
- Lawrence, G. M. (1972b), Photodissociation of CO₂ to produce CO (a³Π), *J. Chem. Phys.*, *56*, 3435.
- Le Teuff, Y. H., T. J. Millar, and A. J. Markwick (2000), The UMIST Database for Astrochemistry 1999, *Astron. Astrophys. Suppl. Ser.*, *146*, 157.
- Lebofsky, L. A. (1975), Stability of frosts in the solar system, *Icarus*, *25*, 205–217.
- Lellouch, E. (1996), Urey Prize Lecture—Io's atmosphere: Not yet understood, *Icarus*, *124*, 1–21.
- Masuoka, T. (1994), Single-photoionization and double-photoionization cross-sections of carbon dioxide (CO₂) and ionic fragmentation of CO₂⁺ and CO₂⁺, *Phys. Rev. A*, *50*, 3886–3894.
- Masuoka, T., and E. Nakamura (1993), Single-photoionization, double-photoionization, and triple-photoionization cross-sections of carbon monoxide (CO) and ionic fragmentation of CO⁺, CO₂⁺, and CO₃⁺, *Phys. Rev. A*, *48*, 4379–4389.
- Masuoka, T., and J. A. R. Samson (1981), Dissociative and double photoionization of CO from threshold to 90-Å, *J. Chem. Phys.*, *74*, 1093–1097.
- McElroy, M. B., and T. M. Donahue (1972), Stability of Martian atmosphere, *Science*, *177*, 986.
- Miller, T. M., R. E. Wetterskog, and J. F. Paulson (1984), Temperature dependence of the ion-molecule reactions N⁺ + CO, C⁺ + NO, and C⁺, CO⁺, CO₂⁺ + O₂ from 90–450 K, *J. Chem. Phys.*, *80*, 4922–4925.
- Moore, J. M., M. T. Mellon, and A. P. Zent (1996), Mass wasting and ground collapse in terrains of volatile-rich deposits as a solar system-wide geological process: The pre-Galileo view, *Icarus*, *122*, 63–78.
- Moore, J. M., et al. (1999), Mass movement and landform degradation of the icy Galilean satellites: Results of the Galileo nominal mission, *Icarus*, *140*, 294–312.
- Moses, J. I., E. Lellouch, B. Bezard, G. R. Gladstone, H. Feuchtgruber, and M. Allen (2000), Photochemistry of Saturn's atmosphere II. Effects of an influx of external oxygen, *Icarus*, *145*, 166–202.
- Mount, G. H., and G. J. Rottman (1983), The solar absolute spectral irradiance 1150–3173 Å—May 17, 1982, *J. Geophys. Res.*, *88*, 5403–5410.
- Mul, P. M., J. W. McGowan, P. Defrance, and J. B. A. Mitchell (1983), Merged electron-ion beam experiments. 5. Dissociative recombination of OH⁺, H₂O⁺, H₃O⁺ and D₃O⁺, *J. Phys. B At. Mol. Phys.*, *16*, 3099–3107.
- Neubauer, F. M. (1998), The sub-Alfvénic interaction of the Galilean satellites with the Jovian magnetosphere, *J. Geophys. Res.*, *103*, 19,843–19,866.
- Okabe, H. (1978), *Photochemistry of Small Molecules*, John Wiley, Hoboken, N. J.
- Pearl, J., R. Hanel, V. Kunde, W. Maguire, K. Fox, S. Gupta, C. Ponnampuruma, and F. Raulin (1979), Identification of gaseous SO₂ and new upper limits for other gases on Io, *Nature*, *280*, 755–758.
- Shaw, D. A., D. M. P. Holland, M. A. Hayes, M. A. Macdonald, A. Hopkirk, and S. M. McSweeney (1995), A study of the absolute photoabsorption, photoionization and photodissociation cross-sections and the photoionization quantum efficiency of carbon dioxide from the ionization threshold to 345-Ångstrom, *Chem. Phys.*, *198*, 381–396.
- Sheehan, C. H., and J.-P. St.-Maurice (2004), Dissociative recombination of N₂⁺, O₂⁺, and NO⁺: Rate coefficients for ground state and vibrationally excited ions, *J. Geophys. Res.*, *109*, A03302, doi:10.1029/2003JA010132.
- Skrzypkowski, M. P., T. Gougousi, R. Johnsen, and M. F. Golde (1998), Measurement of the absolute yield of CO(a³Π) + O products in the dissociative recombination of CO₂⁺ ions with electrons, *J. Chem. Phys.*, *108*, 8400–8407.
- Spencer, J. R., and W. M. Calvin (2002), Condensed O₂ on Europa and Callisto, *Astron. J.*, *124*, 3400–3403.

- Strobel, D. F., J. Saur, P. D. Feldman, and M. A. McGrath (2002), Hubble Space Telescope space telescope imaging spectrograph search for an atmosphere on Callisto: A Jovian unipolar inductor, *Astrophys. J.*, *581*, L51–L54.
- Tan, K. H., C. E. Brion, P. E. Vanderleeuw, and M. J. Vanderwiel (1978), Absolute oscillator strengths (10–60 eV) for photoabsorption, photoionization and fragmentation of H₂O, *Chem. Phys.*, *29*, 299–309.
- Torr, M. R., and D. G. Torr (1985), Ionization frequencies for solar Cycle-21: Revised, *J. Geophys. Res.*, *90*, 6675–6678.
- Van Brunt, R. J., F. W. Powell, R. G. Hirsch, and W. D. Whitehead (1972), Photoionization of N₂, O₂, NO, CO, and CO₂ by soft X rays, *J. Chem. Phys.*, *57*, 3120–3129.
- Vejby-Christensen, L., L. H. Andersen, O. Heber, D. Kella, H. B. Pedersen, H. T. Schmidt, and D. Zajfman (1997), Complete branching ratios for the dissociative recombination of H₂O⁺, H₃O⁺, and CH₃⁺, *Astrophys. J.*, *483*, 531–540.
- Weiss, B. P., Y. L. Yung, and K. H. Nealson (2000), Atmospheric energy for subsurface life on Mars?, *Proc. Natl. Acad. Sci. U. S. A.*, *97*, 1395–1399.
- Weller, C. S., and M. A. Biondi (1967), Measurements of dissociative recombination of CO₂⁺ ions with electrons, *Phys. Rev. Lett.*, *19*, 59.
- Wight, G. R., M. J. Vanderwiel, and C. E. Brion (1976), Dipole excitation, ionization and fragmentation of N₂ and CO in 10–60 eV Region, *J. Phys. B At. Mol. Phys.*, *9*, 675–689.
- World Meteorological Organization (1985), *Atmospheric Ozone*, vol. 1, *Rep. 16*, Geneva.
- Yung, Y. L., and W. B. DeMore (1999), *Photochemistry of Planetary Atmospheres*, pp. 258–260, Oxford Univ. Press, New York.
- Yung, Y. L., and M. B. McElroy (1977), Stability of an oxygen atmosphere on Ganymede, *Icarus*, *30*, 97–103.
-
- M. Allen, Jet Propulsion Laboratory, California Institute of Technology, MS 183-401, 4800 Oak Grove Drive, Pasadena, CA 91109, USA. (maa@gps.caltech.edu)
- B. F. Lane, MIT Center for Space Research, 70 Vassar Street, Cambridge, MA 02139, USA. (blane@mit.edu)
- M.-C. Liang and Y. L. Yung, Division of Geological and Planetary Sciences, California Institute of Technology, MS150-21, 1200 East California Boulevard, Pasadena, CA 91125, USA. (mcl@gps.caltech.edu; yly@gps.caltech.edu)
- R. T. Pappalardo, Laboratory for Atmospheric and Space Physics, University of Colorado, Boulder, CO 80309, USA. (robert.pappalardo@colorado.edu)